Performance Prediction of Waste Polyethylene Gasification Using CO_2 in a Bubbling Fluidized Bed: A Modelling Study

R. D. Alli, P. Kannan, A. Al Shoaibi,* and C. Srinivasakannan
Department of Chemical Engineering, Khalifa University,
P.O. Box 2533. Abu Dhabi. UAE

doi: 10.15255/CABEQ.2018.1384
Original scientific paper
Received: May 22, 2018
Accepted: September 24, 2018

Gasification of carbonaceous materials using CO_2 from flue gases is an effective and economic means of waste recycling and environmental CO_2 mitigation system. The paper presents investigation on conversion of plastics, such as (poly) ethylene, into valuable gaseous products, primarily Syngas or synthesis gas using CO_2 as a gasifying agent instead of conventional steam. Typically, gasification is carried out in a fluidized bed reactor followed by sequential separation of syngas from tar and other undesired gaseous products. In this research work, the effect of operating conditions of the fluidized bed reactor on carbon conversion and H_2/CO mole ratio was examined. For this purpose, a process model of CO_2 gasification of waste plastics using fluidized bed reactor was developed in ASPEN PLUS®. Sensitivity analysis concluded that parameters like CO_2 – feed ratio, residence time, and gasification temperature serve to control the yield and quality of syngas.

Keywords:
fluidized bed reactor, CO_2 gasification, waste LDPE, process modelling

Introduction

Gasification of carbonaceous materials using CO_2 from flue gases is an effective and economic means of waste recycling and environmental CO_2 mitigation system[1]. Recovering energy from waste sources has become essential in order to curtail the burden on the rapidly depleting fossil fuel reserves. On one hand, there is an urgent necessity to minimize CO_2 emissions to negate their impact on global warming, and on the other hand, the issue of waste plastics disposal still remains a major concern. Hence, a process that utilizes CO_2 to recover energy from waste plastics with minimal residue would address both the challenges mentioned above.

Over the decades, many novel technologies have been developed to process plastic wastes into useful products after undergoing certain thermochemical conversion processes. One of the technologies that has attracted widespread attention among researchers and industrialists is gasification. Gasification has the potential to increase the efficiency of power production significantly and produce syngas as a chemical feedstock[2]. Syngas of different H_2/CO ratio could be achieved based on feedstock composition, process conditions including the type of gasifying agent being used. Depending on the H_2/CO ratio in syngas, applications of syngas vary widely, from hydrogen production to transportation fuels[3].

Gasification has been the preferred technology among other available thermochemical conversion methods owing to its relatively greater environmental sustainability and flexibility in process integration for power plants. Conversely, the technique also has a tendency to produce a significant amount of undesired tar, and other inorganics that impede the performance and efficiency of the process. However, such limitations have been addressed successfully through continuous process improvements on the gasification system, including catalyst development, feedstock modification, and reactor configuration improvements.

Gasification processes are carried out in three popular modes of gasifiers; the moving bed or fixed bed gasifier, entrained flow gasifier, and fluidized bed gasifier, and these gasifiers could be downdrafts, cross drafts or updrafts. The advantage of the fluidized bed gasifier is the exceptional mixing and temperature homogeneity, ability to tolerate fine and coarse particles, and relatively low gasification temperature, making it most preferred for gasification[2]. As the feed and the gasifying agent enter the reactor, it mixes easily with the bed material and is very quickly heated up to the bed temperature. Gasification is normally implemented at elevated temperatures (600 °C to 800 °C) in an air-lean environment. Due to the small feed particle size and rapid

*Corresponding author: E-mail: ahmed.alshoaibi@ku.ac.ae
Ph: +971-26075586 Fax: +971-26075200

heating, a portion of the feed instantaneously undergoes pyrolysis, generating char and other volatiles. This is followed by char and volatile gasification, producing syngas, tar, and other hydrocarbons.

Gasification of waste plastics has been attempted since the 1970's, wherein typically steam and air have been used as the gasifying agents[4,5]. Tsuji *et al*.[6] investigated catalytic conversion of oils derived from waste LDPE and PS to Syngas by steam reforming in a fluidized bed. It was concluded that at temperatures above 1023 K and a steam to carbon ratio of 3.5, the product gas recorded almost 70 % hydrogen composition. The use of steam as the gasifying agent yields higher H_2/CO ratio owing to the predominance of steam reforming reactions. This conclusion on the effect of steam on product composition is in good agreement throughout the literature. The composition of the product gas could be vastly different when different gasifying agents other than steam are employed. Ongen[7] conducted gasification experiments on waste plastic samples in the presence of dry air at 750 °C. At these conditions, the producer gas was found to contain high amounts of methane in comparison to hydrogen and CO. Utilization of CO_2 also as a gasifying medium for gasification of coal, biomass and municipal solid waste has been reported in literature[8]. Apart from the environmental advantage, CO_2 offers significant technical benefits, like better char gasification and pyrolysis, improved tar mitigation, and regulating H_2/CO ratio in product stream[9]. More recently, Couto *et al*.[10] presented a numerical model that assessed municipal solid waste gasification using air-CO_2 mixtures. Results demonstrated that increasing rates of CO_2 introduced as part of the gasifying agent enhanced char conversion and increased CO levels. The feasibility of using CO_2 alone as a gasifying agent in the gasification of carbonaceous materials to syngas has also been reported by Parvez *et al*.[8] Results from thermogravimetric analysis showed that CO_2 enhances interactions between the volatiles from individual components, thereby influencing gasification characteristics of the feed mixture.

There is enough experimental data presented in literature that elucidates the influence of CO_2 interaction with biomass and plastic blends. However, a systematic assessment that details the influence of CO_2 interaction and operating conditions on co-mingled waste plastics gasification is not available. Such a report would first mandate a thorough investigation on the gasification characteristics of single plastic component under CO_2 atmosphere using a commercial reactor such as a fluidized bed. A gasification process model would serve to simulate and perform a sensitivity analysis to determine feedstock blend compatibility and optimum conditions for efficient gasification. The aim of this project is to develop a comprehensive process model in ASPEN PLUS® that could be used to simulate CO_2 gasification of waste LDPE in a bubbling fluidized bed. The effect of various hydrodynamic and process parameters would be studied and presented in detail. Furthermore, this study would assist in detailed process design and scale up studies.

Simulation methodology

Most of the previous work on this subject has utilized only a simplified version of the fluidized bed due to the complexity in capturing both the reaction chemistry and reactor hydrodynamics. Even more recently, Beheshti *et al*.[11] simulated biomass gasification in a fluidized bed by substituting CSTR and PFR models to mimic the bed zone and freeboard of the reactor, respectively. However, CSTR and PFR models would not be able to completely account the hydrodynamic parameters of the fluidized bed reactor. It would be challenging to exclude the effects of bubble diameter, bubble rise velocity, bubble volume fraction, transport disengagement height, and interstitial velocity on product gas composition. In a bid to overcome these limitations, a fluidized bed reactor available in ASPEN PLUS® reactor module has been selected in this study. Apart from the hydrodynamic parameters, gasification reactions and their kinetic parameters were provided as input to the model. The major kinetic parameters required for the kinetic model are the activation energy (E_a) and the rate constant (k) for the major reactions. Many authors have reported values for E_a and k for the major gasification reactions based on the rate equation; $r_i = k_i \cdot c_A \cdot c_B$ and the Arrhenius equation; $k = A \exp\left(-E_a / RT\right)$. The set of gasification reactions and their kinetic parameters taken from literature[12–13] are shown in Table 1.

The following technical assumptions were considered in the process model:

1. Isothermal and steady state process.
2. Solids are ideally mixed.
3. The bed comprises of a bubble phase and an emulsion phase. The inlet gas flows through the fluidized bed, split as bubble phase and emulsion phase.
4. Devolatilization is instantaneous, and volatiles consist mainly of CO, H_2, CH_4, CO_2 and H_2O.
5. Within the emulsion phase, gases are uniformly distributed.
6. Char only consist of carbon and ash.
7. Char gasification starts in the bed and is completed in the freeboard.
8. Particles are spherical and the average particle diameter remains constant throughout the gasification based on the shrinking core model.

Table 1 – *List of gasification reactions and their kinetic parameters*

Name	Reaction	Heat of reaction (kJ mol^{-1})	Kinetic Parameters	Ref
Boudouard	$C + CO_2 \rightarrow 2CO$	+172	$0.12\exp(-17921/T)$	11
Char gasification	$C + H_2O \rightarrow CO + H_2$	+131	$2{\cdot}10^5\exp(-6000/T)$	12,22
Hydrogasification	$C + 2H_2 \rightarrow CH_4$	–74.8	$4.4\exp(-1.62{\cdot}10^8/T)$	11
Methane reforming	$CH_4 + H_2O \rightarrow CO + 3H_2$	+206	$3{\cdot}10^5\exp(-15000/T)$	12
Water gas shift	$CO + H_2O \rightleftarrows CO_2 + H_2$	–41.2	$10^6\exp(-6370/T)$ $K_w = 520\exp(-7230/T)$	12,22

Process modelling

The process model developed in ASPEN PLUS® is shown in Fig. 1. The process flow diagram includes dryer, RYIELD reactor, splitters, RGIBBS reactor, mixers, and the fluidized bed reactor. Details of the stream and models are outlined below.

– WETHDPE: This stream contains the polyethylene feed, which was defined as a polymer at room temperature with a flowrate of 1200 kg h^{-1}. It was defined as a non-conventional component with the ultimate and proximate analysis as specified in Table 2.

– DRYER: The dryer was operated at 100 °C and 1 bar in order to implement the first stage of gasification, which is the drying process of the feed. Water evaporated from the polyethylene feed goes to the 'EVAPH2O' stream, while the dried feed goes to the 'DRYPE' stream.

– DECOM: Pyrolysis of the dry feed is modelled in the RYIELD reactor. In this reactor, polyethylene is converted into its constituting components, which include carbon, hydrogen, oxygen, nitrogen, sulphur, and ash, by specifying the yield distribution according to the ultimate analysis. The operating conditions are 1 atm and 400 °C, and the products of the reactor consist of volatiles and char exiting at a preheated temperature of 400 °C.

Table 2 – *PE proximate and ultimate analysis of LDPE*[16]

Proximate analysis				Ultimate analysis					
MC	VM	FC	ASH	C	H	N	S	O	ASH
0.02	99.85	0	19.78	80.7	14.0	0.06	0.08	5.2	19.8

– B6-SPLITTER: This splitter models separation of the volatile materials from carbon. The amount of volatile materials was taken from the proximate analysis under the assumption that char contains only carbon and ash.

– RGIBBS: RGIBBS reactor is based on the Gibbs free energy minimization theory. It is operated at the same temperature and pressure of the fluidized bed, and it models the devolatilization stage of the gasification process. All possible gaseous components are specified as an input in this reactor module.

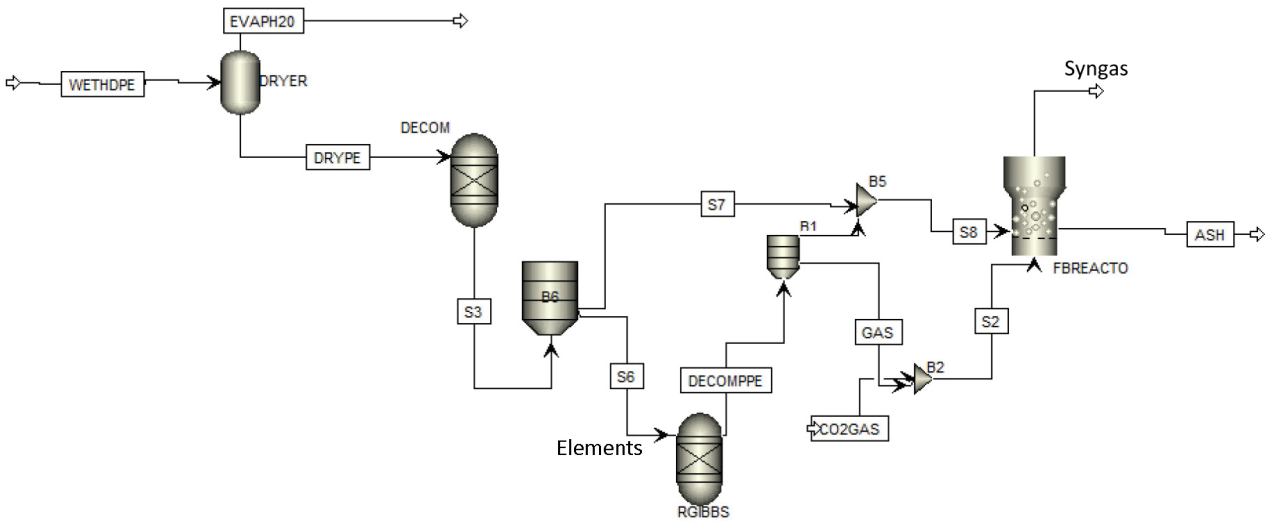

Fig. 1 – *Simulation model of the gasification process*

– R1-SPLITTER: The products of the RG-IBBS reactor, 'DECOMPPE' enter this splitter that separates the solids from the gas. This is essential as the entry points of solids and gases into the fluidized bed reactor are different.

– CO_2 GAS: The gas stream contains CO_2 at a temperature of 400 °C at 1.5 bar pressure. CO_2 serves as the gasifying agent required to drive the gasification process. It enters mixer-B2 along with other volatiles, which are then passed to the bottom of the fluidized reactor.

– FBREACTOR: The 'FBREACTOR' is an inbuilt reactor module in ASPEN PLUS® that can be used for modelling fluidized beds with or without reactions. The fluidized bed is distinguished into two zones: the bottom zone characterized by high solids volume concentrations, and the upper dilute zone in which the solids concentration decreases with increasing height. The total height of the reactor is the sum of bottom zone and the upper dilute zone. The bottom zone is modelled as a bubbling bed according to Werther and Wein[14], and for the description of the upper dilute zone an approach according to Kunii and Levenspiel[15] was used. Geldart B particle classification with average particle diameter of 167.5 mm, bed mass of 1600 kg, and a voidage of 0.4 at minimum fluidization was considered. The gasification reactions along with the kinetics detailed earlier were specified in the fluidized bed module. In addition to reactor configuration and operating conditions, gas distributor type, orifice dimensions, and discharge coefficient were also specified in the module. A few relevant equations used to describe the model are discussed in the next section.

Fluidized bed governing equations

Some of the relevant governing equations of the fluidized bed employed in ASPEN PLUS® to calculate hydrodynamic properties are discussed below.

Minimum fluidization velocity (u_{mf})

ASPEN PLUS® calculates minimum fluidization velocity by assuming that the pressure drop in flow through the poly-disperse fixed bed, as given by Ergun equation, equals the solids pressure drop, and thus,

$$u_{\mathrm{mf}} = 7.14 \cdot \left(1-\varepsilon_{\mathrm{mf}}\right) \cdot \gamma_{\mathrm{f}} \cdot S_{\mathrm{v}} \cdot \left[\sqrt{1 + 0.067 \cdot \frac{\varepsilon_{\mathrm{mf}}^3}{\left(1-\varepsilon_{\mathrm{mf}}\right)^2} \cdot \frac{\left(\rho_{\mathrm{s}} - \rho_{\mathrm{f}}\right) \cdot g}{\rho_{\mathrm{f}} \cdot \gamma_{\mathrm{f}}^2} \cdot \frac{1}{S_{\mathrm{v}}^3}} - 1 \right] \qquad (1)$$

Accordingly, to calculate u_{mf}, gas density and viscosity (ρ_f, γ_f), particle density (ρ_s), bed porosity at minimum fluidization (ε_{mf}), and the volume-specific surface area (S_v) must be known.

Bubble diameter (d_v)

The bottom zone is modelled as a bubbling fluidized bed and is assumed that the region consists of two phases, a dense and a void phase. The void phase is made up of bubbles assumed to be solid free. The bubble diameter along the bed height (h) is given by:

$$\frac{\mathrm{d}\left(d_{\mathrm{v}}\right)}{\mathrm{d}h} = \left\{ \frac{2 \cdot \varepsilon_{\mathrm{b}}}{9 \cdot \pi} \right\}^{1/3} - \frac{d_{\mathrm{v}}}{3 \cdot \omega \cdot u_{\mathrm{b}}} \qquad (2)$$

The initial diameter of the bubble from the distributor plate is based on Davidson and Harrison correlation, which is given by:

$$d_{\mathrm{vo}} = 1.3 \cdot \left(\frac{V_{\mathrm{or}}^2}{g} \right)^{0.2} \qquad (3)$$

where V_{or} is the volumetric flowrate of the gas through an orifice, ω is mean life of bubble that is calculated from $\omega = 280 \cdot \frac{u_{\mathrm{mf}}}{g}$, ε_b is the local bubble volume fraction, and u_b is the local bubble rise velocity.

Transport disengagement height (TDH)

The distance between the point where the solids concentration is nearly constant and the surface of the fluidized bed is called the transport disengagement height (TDH). Several correlations for the determination of TDH are available in ASPEN PLUS® but the George and Grace correlation shown below was utilized in this work.

$$\mathrm{TDH} = 18.2 \cdot d_{\mathrm{b}} \qquad (4)$$

where d_b refers to the bubble diameter at the surface of the bed. In the simulator, if the calculated height of the freeboard is smaller than the TDH, a warning is issued.

Elutriation

The bottom zone of the reactor that is modelled as a bubbling fluidized bed is assumed to be homogeneously distributed with particles. When the bub-

bles explode at the bed surface, some of the fines are sputtered out into the freeboard, finally resulting in transport of particles by the gas stream. If the freeboard height is higher than TDH, the elutriated mass of solids depends on the particle terminal velocity, gas velocity, and the solid mass fraction. The elutriated mass flow $\dot{m}_{e,i}$ of a particle possessing terminal velocity 'i' is given as:

$$\dot{m}_{e,i} = K_{\infty,i} \cdot A_t\left(H_b\right) \cdot \Delta Q_{3,b,i} \tag{5}$$

where $K_{\infty,i}$ is a particle-related elutriation coefficient, $\Delta Q_{3,b,i}$ is the mass fraction of particles of terminal velocity i in the total mass inventory, $A_t(H_b)$ is the cross-sectional area of the bubbling bed at the actual bed height (H_b). There are a few correlations available for the calculation of particle-related elutriation coefficient, however in this model, the correlation proposed by Zenz and Weil[16] was employed.

$$K_{\infty,i} = A \cdot \varphi^b \tag{6}$$

and

$$\varphi = \left\{ \frac{u^2}{g \cdot d_{p,i} \cdot \rho_{S,i}^2} \right\} \tag{7}$$

$$for\ \varphi < 3.0 \cdot 10^{-4} : A = 1.26 \cdot 10^7; b = 1.88$$

$$for\ \varphi > 3.0 \cdot 10^{-4} : A = 1.31 \cdot 10^4; b = 1.18\,.$$

Superficial gas velocity

The superficial gas velocity $u_g(h)$, at a height "h" in the fluidized bed is determined based on the mass flow of vapour (m_g) at that height, the density of the vapour phase $\rho_g(T, p(h))$, and the cross-sectional area $A(h)$ of the reactor at the given height. It is given by:

$$u_g\left(h\right) = \frac{m_g}{\rho_g\left(T, p\left(h\right)\right) \cdot A\left(h\right)} \tag{8}$$

Pressure drop across the bed

The pressure drop of the fluid passing through a fluidized bed is equal to the total weight of the suspension per cross-sectional area of the bed, and is given by:

$$\Delta p_{fb} = H \cdot \left(1 - \varepsilon\right) \cdot \left(\rho_s - \rho_g\right) + H \cdot \varepsilon \cdot \rho_f \cdot g \tag{9}$$

where ε is the bed porosity, and g is acceleration due to gravity.

Pressure drop across the distributor

The pressure drop of the gas distributor Δp_{dis} is given as

$$\Delta p_{dis} = \left[\frac{u_{or}}{C_{dis}}\right]^2 \cdot \frac{\rho_f}{2} \tag{10}$$

where u_{or} denotes the fluidization gas velocity within an orifice, C_{dis} is the orifice discharge coefficient, and ρ_f is the density of the fluidization gas. Other details on input specifications and equations can be found in ASPEN PLUS® manual.

In this work, a semi-detailed kinetic method has been developed that models devolatilization (pyrolysis) process assuming complete equilibrium, while the gasification processes are built on kinetic based models. The effect of process parameters on the equilibrium process is not part of this study, and is assumed to not vary significantly in the parametric range considered.

Results and discussion

In this work, a process model of CO_2 gasification of LDPE using a bubbling fluidized bed has been developed in ASPEN PLUS®. This model was utilized for a parametric investigation of the process parameters on syngas quality and carbon conversion. The effects of hydrodynamic parameters and operating conditions, such as the gasification temperature, CO_2 to feedstock ratio, gas flowrate, height, and diameter of reactor, distribution plate free area, distributor plate perforation diameter, and flowrate of carbon were assessed on H_2/CO molar ratio in the product gas and carbon conversion. The results were analysed in lieu of bed hydrodynamics and reaction dynamic equilibrium conditions.

Effect of gasification temperature

The effect of gasification temperature on syngas distribution and carbon conversion was assessed in the range of 750 °C to 950 °C. In the simulation model, the temperature of the fluidized bed was varied, while all other model parameters were held constant at specific conditions listed in Table 3.

Table 3 – *Base case operating conditions for sensitivity analysis*

Operating conditions	
Height of reactor (m)	19
Diameter of reactor (m)	2
Diameter of orifice (mm)	2
Flow rate of carbon (kmol h^{-1})	40
Flow rate of CO_2 (kmol h^{-1})	70
Number of orifices	10000

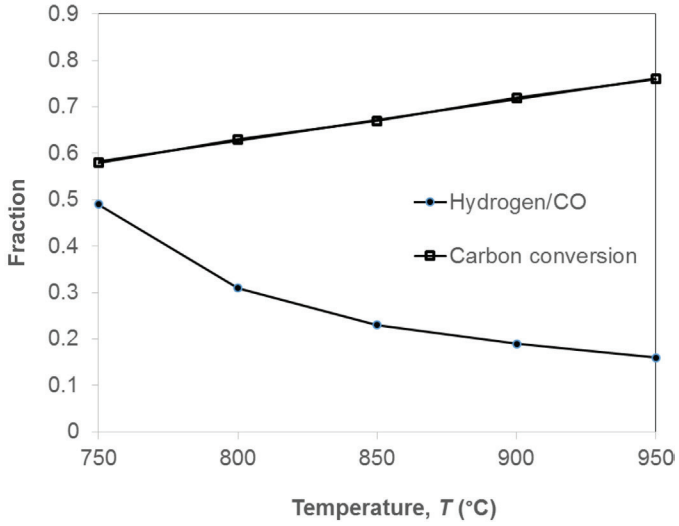

Fig. 2 – *Effect of gasification reactor temperature on syngas quality and carbon conversion*

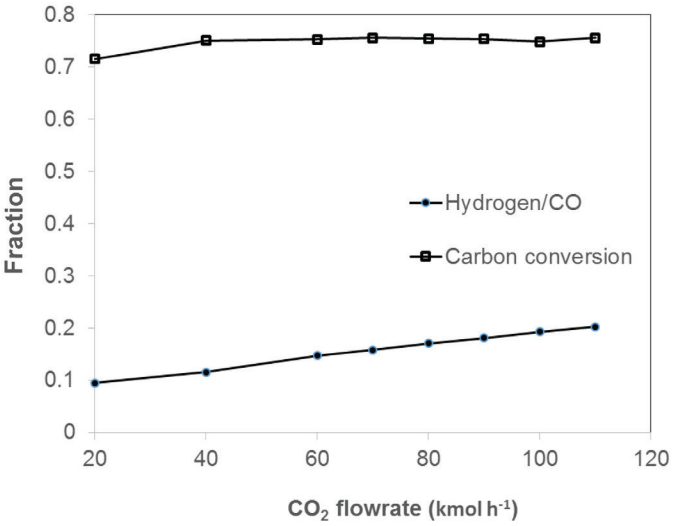

Fig. 3 – *Effect of gasifying agent CO_2 flow rate on syngas quality and carbon conversion*

It can be noticed from Fig. 2 that, with an increase in temperature from 750 °C to 950 °C, carbon conversion increased from 59 % to 77 % with simultaneous decrease in H_2/CO ratio from 50 % to 18 %. During this time, it was observed that the output rate of CO increased significantly from 16 to 44 kmol h^{-1} with a negligible change in hydrogen and methane flows. In contrast, when steam was used as the gasifying medium, the methane-reforming reaction was found to be dominant, resulting in higher hydrogen formation, thus increasing the H_2/CO ratio[11]. Although the pyrolysis of plastics involves breaking of C-C and C-H bonds to form smaller molecules, CO_2 does not react with these hydrocarbon fragments[17]. Hence, the major mechanism that contributes to a higher generation of CO and higher carbon conversion is possibly the Boudouard reaction. Being a highly endothermic reaction, an increase in temperature drives the forward reaction, thereby increasing conversion of carbon and production of CO. This would also contribute to the reduction in CO_2 due to higher consumption of carbon in the reaction. In addition, the exothermic nature of the water-gas shift reaction would favourably shift the reaction to the left, contributing to the increased levels of CO and H_2O in product stream. Moreover, an increased temperature specific to fluidized beds can be attributed to the reduction in the emulsion phase surface tension leading to an increase in solid mixing and diffusivity between the phases contributing to enhanced transfer rates[18–19].

Effect of CO_2 – carbon feed ratio

From the list of various gasification reactions listed in Table 1 and through literature review on CO_2 gasification, the gasifying agent – feed ratio is known to be a major factor that would affect the product conversion and product distribution. In order to assess the effect of gasifying medium flow rate, simulations were run at various CO_2 flow rates between 20 and 110 kmol h^{-1} with a corresponding CO_2 to feed ratio between 0.5 and 2.75, keeping other parameters constant at the base case conditions.

Fig. 3 depicts the influence of CO_2 flow rate on carbon conversion and syngas composition. An initial increase in conversion from 70 % to 75 % with increase in CO_2 flow rate could be attributed to the Boudouard reaction that favours the generation of CO through consumption of carbon in the reactor. Additionally, the increase in carbon conversion can also be due to the hydrogasification reaction with hydrogen leading to methane formation, which increases from 34.5 % to 38 %. Beyond a CO_2 flow rate 40 kmol h^{-1}, although the molar ratio of H_2/CO steadily increases, carbon conversion remains constant. During this time, CO flow rate remained constant at 43 kmol h^{-1}, while hydrogen marginally increased from 5 to 8.5 kmol h^{-1}. When the stoichiometric CO_2 limit has been reached, both the methanation and Boudouard reaction do not proceed further, resulting in continual increase of unreacted CO_2 concentration in the product stream.

With respect to the hydrodynamics of fluidized bed, an increase in the flow rate of gasifying medium would facilitate a larger proportion of the gas bypassing the bed as bubbles, thereby increasing bed voidage and possibly contributing to reduced mass transfer rates. In addition, at higher gas flow rates, the effective residence time of the bubbles in the bed would be less due to larger bubble size and larger bubble fraction in the bed, both contributing to a reduction in carbon conversion[16,18].

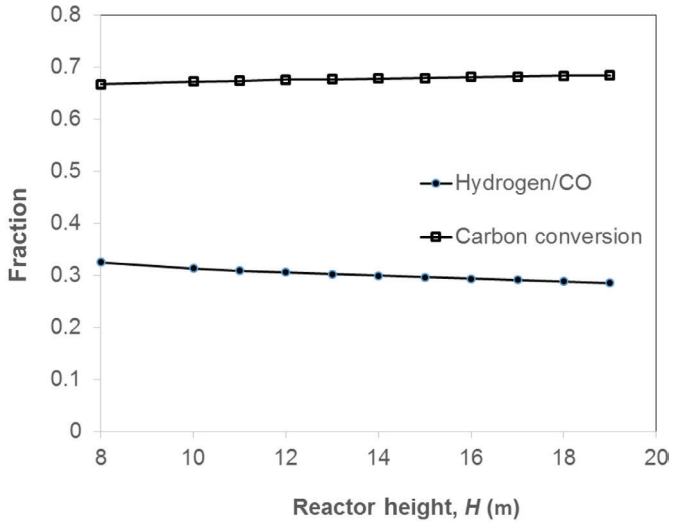

Fig. 4 – *Effect of reactor height on syngas quality and carbon conversion*

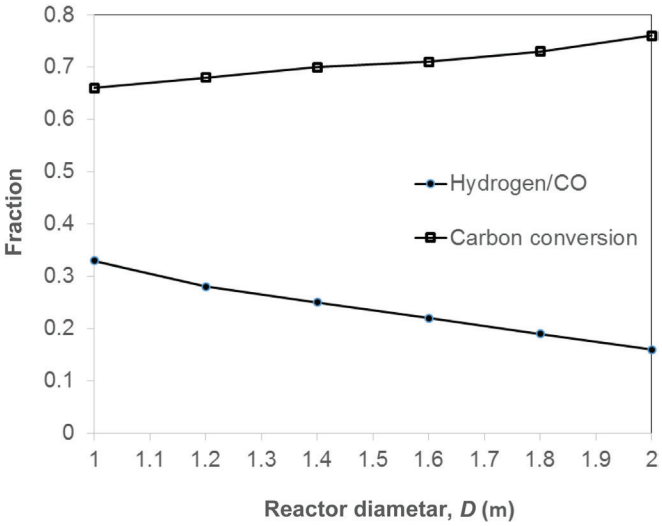

Fig. 5 – *Effect of bed diameter on syngas quality and carbon conversion*

Effect of reactor height

The height of the reactor was varied between 8 m and 19 m in order to assess the effect on carbon conversion and syngas generation. Increasing the reactor height would increase the residence time of the product gases, allowing the gasification reactions to continue for an extended time[20–22]. Hence, an increased extent of gasification reaction could be expected with increasing reactor heights. Fig. 4 illustrates the variation of syngas quality and carbon conversion with overall height of the fluidized bed. With an increase in reactor height from 8 m to 19 m, H_2/CO ratio slightly decreased from 0.32 to 0.28, while carbon conversion remained constant at about 66 %. This was because, although total reactor height increased, neither the bed height (bottom zone) wherein solid carbon was present, nor the transport disengagement height (TDH) varied, hence, the conversion remained unchanged. The molar flow of CO was found to increase slightly from 30.6 to 33.1 kmol h^{-1}, thus reducing the H_2/CO ratio.

Effect of reactor diameter

With increasing bed diameter, the size of the gasifying medium distributor plate at the bottom of the bed would increase. However, to maintain a constant distributor free area, the number of orifices on the distribution plate was adjusted in each test case, keeping other reactor geometric and configuration parameters constant. Fig. 5 shows the variation of syngas composition and carbon conversion as a function of reactor diameter ranging between 1 m and 2 m, while the number of orifices changed from 400 to 1600. A decrease in H_2/CO mole ratio from 0.33 to 0.15 and an increase in carbon conversion from 66 % to 76 % can be observed with increasing reactor diameter.

Increasing the number of orifices leads to an increase in the number of bubbles of smaller diameter, however, at a lesser frequency for a fixed gas flow rate. An increased surface area and hence an enhanced exchange rate between the bubble phase and emulsion phase would lead to a higher carbon conversion, which would consequently generate a higher amount of CO in syngas composition due to the Boudouard reaction. Additionally, the residence time for the gas-solid reaction would increase with an increase in the bed diameter, contributing to higher carbon conversion[23].

Effect of distributor free area

The distributor free area is the extent of free space available on the gas distributor plate for the gasifying medium to pass before entering the bed. Two cases of 5 % and 10 % free area were considered at a temperature of 950 °C, orifice diameter of 2 mm, gas flow rate of 70 kmol h^{-1}, and the number of orifices in each case was varied. It can be noticed from Table 4 that with increasing free area, H_2/CO

Table 4 – *Effect of distributor free area on product composition*

	10 % free area	5 % free area
Carbon conversion (%)	75.59	69.94
CO (kmol h^{-1})	43.97	35.63
CH_4 (kmol h^{-1})	37.57	36.78
H_2 (kmol h^{-1})	6.97	9.34
H_2O (kmol h^{-1})	1.09	0.31

ratio decreased with a simultaneous increase in carbon conversion. For a fixed cross-sectional area of the plate and constant gas flow rate, a higher number of orifices (10 % free area) would yield a low volumetric flow rate per orifice relative to the 5 % free area. Lower gas flow rate would thereby yield a lower initial bubble diameter which would engender a lower bubble diameter/size. On the contrary, in the case of 5 % free area, the number of orifices is relatively lower, resulting in higher bubble formation frequency and increased bubble velocity. Larger bubble size relates to a lower heat and mass transfer rate, and therefore lower carbon conversion and a higher H_2/CO ratio.

The above explanation could be further supported by considering the equations of the bubble diameter utilized in the fluidized bed reactor. At constant values of bed cross-sectional area (A_t) and superficial gas velocity (U_g), a higher number of orifices (n_{or}) would yield a lower value of volumetric flow rate of gas per orifice (V_{or}) and lower velocity as per equations (11) and (12). A lower flow rate would thereby yield a lower initial bubble diameter (D_{bo}) as shown in Eq. (3) which would stimulate a lower bubble diameter/size (D_b) as expressed in the equations below.

$$u_{or} = \frac{V}{n_{or} \cdot \frac{\pi d_{or}^2}{4}} \tag{11}$$

$$V_{or} = \frac{U A_t}{n_{or}} \tag{12}$$

$$D_b = 2.05\left(U - U_{mf}\right)^{0.94} h + D_{bo} \tag{13}$$

Effect of distributor orifice diameter

In order to understand the influence of plate orifice diameter on the product gas quality and carbon conversion, simulations were performed by varying orifice diameters from 2 mm to 10 mm, keeping all other parameters fixed. This would permit to study the effect of bubble diameter on the gasification process. With increasing orifice diameter, volumetric flow rate per orifice will increase and subsequently result in a higher bubble diameter. However, unlike the previous case, where the number of orifices varied in the order of 100's and resulted in a significant change in bubble diameter, the change in orifice diameter in this study is relatively very small. Hence, the effect of orifice diameter on syngas quality and carbon conversion is minimal.

Effect of carbon flow rate

Carbon flow rate refers to the amount of carbon that is available for gasification reactions resulting from pyrolysis products (B6 SPLITTER). Since the elemental composition remains constant, the carbon flow rate was varied by directly changing the plastics feed rate into the system. The influence of the flow rate of carbon ($\dot{F}$) on the composition of syngas and carbon conversion was studied, and the results are shown in Fig. 6. A decrease in carbon conversion from 76 % to 44 % and CO generation from 44 to 32 kmol h^{-1} can be noticed when the carbon flow rate was varied from 40 to 72 kmol h^{-1}. An increase in carbon flow rate resulted in reduced carbon conversion, and hence a decrease in the amount of CO generated. An increase in the carbon flow rate at a fixed CO_2 flow rate would stoichiometrically limit the availability of CO_2 for carbon conversion at high carbon flow rates, and hence reduce the conversion. Furthermore, an increase in carbon flow rate would additionally result in reduced carbon residence time that would lower conversion.

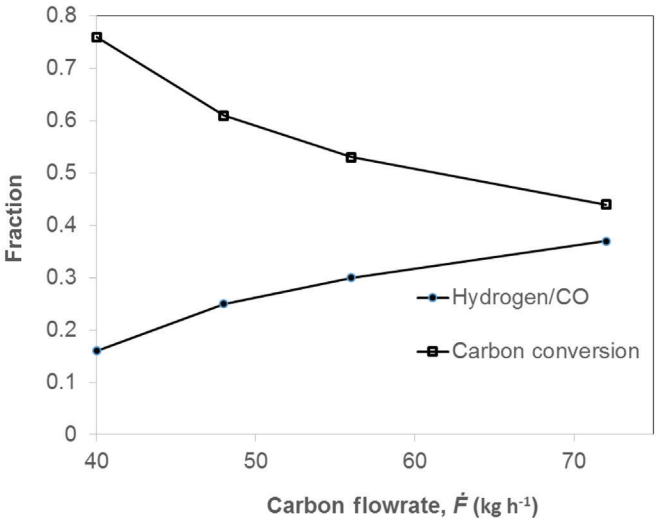

Fig. 6 – *Effect of carbon flowrate on syngas quality and carbon conversion*

Conclusions

The aim of this work is to develop a gasification process model in ASPEN PLUS® that could be used to simulate CO_2 gasification of waste polyethylene in a bubbling fluidized bed. The effects of process conditions and hydrodynamic parameters on carbon conversion and H_2/CO ratio was assessed carefully. An increase in gasification temperature, reactor height, and reactor diameter all resulted in a higher carbon conversion and a lower H_2/CO ratio. In addition, a higher bubble diameter or a decrease in distributor free area decreased carbon conversion and increased the H_2/CO ratio. An increase in the flow rate of carbon entering the fluidized bed has also shown to decrease carbon conversion and increase the H_2/CO ratio. The simulation model de-

veloped in this work is generic in terms of feed handling, and thus serves as a template for studying gasification of other carbonaceous fuels.

Nomenclature

A – Frequency factor
Ar – Archimedes number
C_d – Orifice discharge coefficient
D – Diameter of reactor (m)
d_v – Bubble diameter (m)
D_{b0} – Initial bubble diameter (m)
D_{or} – Diameter of orifice (mm)
d_p – Diameter of particles (μm)
E_a – Activation energy (kJ mol^{-1})
g – Acceleration due to gravity (m s^{-2})
H – Height of reactor (m)
h – Height of reactor bed (m)
M – Mass of particles in bed (kg)
M_g – Mass flow rate of gas (kg min^{-1})
n – Order of reaction
n_{or} – Number of orifices
P – Bed pressure (atm)
R – Universal gas constant (8.314 J K^{-1} mol^{-1})
Re_{mf} – Reynolds number at minimum fluidized bed
S_b – Cross-sectional area of bed (m^2)
TDH – Transport disengagement height (m)
T_0 – Initial temperature (K)
T – Temperature (K)
u_g – Superficial gas velocity (m s^{-1})
u_b – Local bubble rise velocity (m s^{-1})
u_{mf} – Minimum fluidization velocity (m s^{-1})
U_t – Terminal velocity (m s^{-1})
V_{or} – Volumetric flow rate of gas (m^3 s^{-1})
W_0 – Initial sample weight (mg)
W_t – Weight of sample at time t (mg)
W_f – Final weight of sample (mg)
X_i – Mass fraction of sieve at interval i
$\dot{F}$ – Mass flow rate of carbon (kg h^{-1})
S_v – Volume specific surface area (m^2 m^{-3})

Greek letters

α – Conversion
β – Heating rate (K min^{-1})
ε – Bed voidage
γ_f – Viscosity of gas (kg m^{-1} s^{-1})
ρ_b – Bulk density (kg m^{-3})
ρ_g – Gas density (kg m^{-3})
ρ_s – Density of solid (kg m^{-3})
Ø – Sphericity
$\dot{m}_{e,i}$ – Elutriated mass flow rate of particle "i"
ω – Mean life of bubble
ε_b – Local bubble volume fraction

References

1. *Yang, F., Hu, Y., Zhou, F., Chen, D.*, A comparison between CO_2 gasification of various biomass chars and CO_2 gasification of coal char, Sixteenth International Waste Management and Landfill Symposium, CISA Publisher, Italy, 2017.
2. *Quaak, P., Knoef, H., Stassen, H.,* Energy from Biomass: A review of combustion and gasification technologies, World Bank Technical Paper (no. WTP 422) Energy series Washington, D.C. The World Bank, 1999. doi: http://documents.worldbank.org/curated/en/936651468740985551/Energy-from-biomass-a-review-of-combustion-and-gasification-technologies
3. *Luque, R., Speight, J.,* Gasification for Synthetic Fuel Production: Fundamentals, Processes and Applications, Ed. 1, Woodhead Publishing, United Kingdom, 2014.
4. *Buekens, A. G.,* Resource recovery and waste treatment in Japan, Res. Recov. Cons. **3** (1978) 275.
5. *Hasegawa, M., Fukuda, X., Kunii, D.*, Gasification of solid waste in a fluidized bed with circulating sand, Conserv. Recy. **3** (1974) 143. doi: https://doi.org/10.1016/0361-3658(79)90004-3
6. *Tsuji, T., Hatayama, A.,* Gasification of waste plastics by steam reforming in a fluidized bed, J. Mater. Cycles. Waste Manag. **11** (2009) 144. doi: https://doi.org/10.1007/s10163-008-0227-z
7. *Ongen, A*., Methane-rich syngas production by gasification of thermoset waste plastics, Clean Techn. Environ. Policy **18** (2015) 915. doi: https://doi.org/10.1007/s10098-015-1071-1
8. *Parvez, A. M., Mujtaba, I. M., Pang, C., Lester, E., Wu, T.,* Effect of the addition of different waste carbonaceous materials on coal gasification in CO_2 atmosphere, Fuel Proces. Tech. **149** (2016) 231. doi: https://doi.org/10.1016/j.fuproc.2016.04.018
9. *Butterman, H. C., Castaldi, M. J.*, CO_2 as a carbon neutral fuel source via enhanced biomass gasification, Environ. Sci. Technol. **43** (2009) 9030. doi: https://doi.org/10.1021/es901509n
10. *Couto, N., Silva, B., Rouboa, A.*, Municipal solid waste gasification in semi-industrial conditions using air-CO_2 mixtures, Energy **104** (2016) 42. doi: https://doi.org/10.1016/j.energy.2016.03.088
11. *Beheshti, S. M., Gahassemi, H., Shahsavan-Markadeh, R.*, Process simulation of biomass gasification in a bubbling fluidized bed reactor, Energy Cons. Manag. **94** (2015) 345. doi: https://doi.org/10.1016/j.enconman.2015.01.060
12. *Choi, Y. C., Li, X. Y., Park, T. J., Kim, J. H., Lee, J. G.*, Numerical study on the coal gasification characteristics in an entrained flow coal gasifier, Fuel **80** (2001) 2193.
13. *Corella, J., Sanz, A*., Modelling circulating fluidized bed biomass gasifiers. A pseudo-rigorous model for stationary state, Fuel **86** (2005) 1021.
14. *Werther, J., Wein, J*., Expansion behavior of gas fluidized beds in the turbulent regime, AIChE Symp. Ser. **301** (1994) 31.
15. *Kunii, D., Levenspiel, O*., Fluidization Engineering, 2nd ed., Butterworth-Heinemann, U.S.A., 2013.
16. *Yang, W. C*., Handbook of fluidization and fluid-particle systems, Marcel Dekker Inc Pennsylvania, U.S.A, 2003. doi: https://doi.org/10.1201/9780203912744
17. *Tianju, C., Wua, J., Zhang, Z., Zhu, M., Sun, L., Wu, J., Dongke, Z.*, Key thermal events during pyrolysis and CO_2-gasification of selected combustible solid wastes in a thermogravimetric analyser, Fuel **137** (2014) 77. doi: https://doi.org/10.1016/j.fuel.2014.07.077

18. *Abdelgawad, B*., Design of a gas-solid fluidized bed reactor at high temperature and high pressure, Department De Genie Chimique, Universite De Montreal, Ecole Polytechnique De Montreal, 2013.
19. *Sahoo, B*., The effect of parameters on the performance of a fluidized bed reactor and gasifier, National Institute of technology, Rourkela, 2011.
20. *Caterina, G. P., Vilela, A. C. F., Zen, L. D*., Fluidized bed modeling applied to the analysis of processes: Review and state of the art, J. Mat. Res. Tech. **4** (2015) 208. doi: https://doi.org/10.1016/j.jmrt.2014.10.018
21. *Wandeley, P*., Modeling and simulation of an oxychlorination reactor in fluidized bed for the production of 1,2-dichloroethane, Universidade Federal de Alagaos, Portugal, 2010.
22. *Farshi, A., Houman, J., Hamzavi–Abedi, M. A*., An investigation of the effect of bubble diameter on the performance of gas-solid fluidized bed reactor and two-phase modeling of bubbling fluidized bed reactor in melamine production, Pet. & Coal **50** (2008) 11.
23. *Inayat, A., Ahmad, M. M., Yusup, S., Ibrahim, M., Mutalib, A*., Biomass steam gasification with in-situ CO_2 capture for enriched hydrogen gas production: A reaction kinetics modelling approach, Energies **3** (2010) 1472. doi: https://doi.org/10.3390/en3081472